Assessment of Skeletal Muscle Viability by PET

Gary T. Smith, Timothy S. Wilson, Kathryn Hunter, Myrwood C. Besozzi, Karl F. Hubner, David B. Reath, Mitchell H. Goldman and Edward Buonocore

Biomedical Imaging Center, Department of Radiology, and Department of Surgery, University of Tennessee Medical Center, Knoxville, Tennessee

We investigated the use of [^{18}F]fluoro-2-deoxyglucose (FDG) PET scanning for assessment of skeletal muscle viability in patients with peripheral vascular disease and in patients following free-flap skeletal muscle transfer for closure of open wounds. **Methods:** We obtained 32 FDG-PET scans from 30 patients, either at the time of admission for peripheral vascular disease (n = 16) or between 1 and 15 days after surgery for skeletal muscle transfer (n = 16). Ratios between injured and contralateral limb FDG tracer activity uptake were correlated with clinical outcome at 1 mo to 3 yr follow-up. **Results:** Viable muscle uptake ratios ranged from 0.47 to 7.88 (mean: 2.26 ± 1.81; n = 26), while nonviable muscle uptake ratios ranged from 0.12 to 0.46 (mean: 0.27 ± 0.12; n = 6; p < 0.02). After skeletal muscle transfer, two patients with viable tissue, as documented by PET, required amputation due to osteomyelitis, and one patient with peripheral vascular disease who showed viable tissue by PET required amputation 3 mo after the PET scan because of recurrent ulcers. **Conclusion:** FDG-PET scanning can determine skeletal muscle viability in patients with peripheral vascular disease and in patients following free-flap transfer.

Key Words: skeletal muscle viability; positron emission tomography; glucose metabolism; open wound closure

PET has emerged as a promising technique for assessing tissue viability by using radiolabeled glucose to determine the metabolic status of tissue. A PET scanner generates cross-sectional images of radiotracer concentration. Most work has been directed toward using PET for determining myocardial viability following myocardial infarction, estimating glucose metabolic activity in neoplasms and assessing cerebral glucose utilization. Because of the role of glucose as a substrate for anaerobic glycolysis in ischemic muscle, we proposed using [^{18}F]fluoro-2-deoxyglucose (FDG) PET to study muscle viability in trauma and in peripheral vascular disease.

In a pilot study designed to determine whether FDG-PET could visualize injured skeletal muscle, we studied nine trauma patients in the immediate post-trauma period.

Retrospective analysis of the images yielded three patterns of FDG activity distribution in the patients studied:

1. Enhanced uptake of FDG in the acute postinjury phase.
2. Decreased uptake of FDG in the affected muscle.
3. Decreased uptake of FDG in deep muscle with enhanced tracer uptake in the overlying skin.

Five patients with an image pattern showing enhanced metabolism and flow had uneventful hospital courses with healing of their wounds. Three patients with depressed uptake required surgical debridement or amputation. In one patient, a lesion that 'demonstrated a pattern of enhanced skin activity overlying abnormal deep tissue in the posterior lower leg healed after a prolonged treatment course that included hyperbaric oxygen therapy.

In this study, we investigated the use of FDG-PET scans to evaluate skeletal muscle viability in patients with soft-tissue ulcers or other complications of peripheral vascular disease, and in patients after skeletal muscle transfer grafts for closure of open wounds.

MATERIALS AND METHODS

Thirty patients (aged 15 to 90 yr), recently hospitalized for complications of peripheral vascular disease or after skeletal muscle transfer flap surgery, were referred for PET evaluation of skeletal muscle viability. Patients with skeletal muscle transfer grafts were referred for PET evaluation of viability up to 15 days following surgery (Table 1). Two patients who had skeletal muscle transfer underwent scanning in both the early and late postoperative periods. No patients underwent other radionuclide blood flow or blood-pool imaging procedures (e.g., intradermal ^{133}Xe).

FDG was prepared using the method described by Padgett et al. (*1*). Tests for isotopic purity, radiochemical purity, sterility and pyrogenicity were performed for all FDG doses. All patients gave informed consent for the procedure, which was conducted in accordance with guidelines by the Radiation Dosimetry and Safety Committee and the Institutional Review Board of our institution. Scans were obtained on a Siemens ECAT 931 or 921 PET system (Siemens Gammasonics, Hoffmann Estates, IL) between October 1988 and January 1993. Transmission scans were used for attenuation correction. Emission images were obtained 45 min after intravenous injection of 370 MBq (10 mCi) FDG. Images were analyzed by visual inspection of FDG activity distribution on both axial and reformatted coronal and sagittal view emission images. When wounds were too large for complete inclusion in the PET camera's axial field of view, only a specific

TABLE 1
Patients Who Had Skeletal Muscle Transfer

Patient no.	Age (yr)	Sex	Injury	Surgical procedure	Days postop	Glucose (mg/dl)	Uptake ratio	Clinical outcome
1	48	M	Open right tibia pylon fx	Rect + STSG	3	80	2.72	Viable
					10		2.20	Viable
2	35	M	Open midtibia/fibula fx	Rect + STSG	15	93	0.73	Viable
3	55	M	Nonhealing ulcer anterior tibia	LDM	13	69	0.12	Nonviable*
4	21	M	Open distal tibia fx	Rect + STSG	2	125	1.77	Viable†
5	33	M	Open distal tibia fx	Rect + STSG	6	87	2.05	Viable
6	16	M	Open left calcaneal fx	Rect + STSG	5	82	3.47	Viable
7	39	M	Open right tibia fx	LD + STSG	4	122	3.35	Viable
8	15	M	Open left tibia/fibula fx	LDM	2		2.82	Viable
9	53	M	Open right tibia/fibula fx	Rect + STSG	7		2.85	Viable‡
10	21	M	Open right ankle fx/dislocation	Rect + STSG	3	98	5.40	Viable
11	38	M	Osteomyelitis left heel	Rect + STSG	1		6.93	Viable
					6	111	2.00	Viable
12	34	M	Open right tibia/fibula fx	Rect + STSG	1	102	7.88	Viable
13	22	M	Crush right forefoot	LDM	5		1.98	Viable
14	37	M	GSW left popliteal fossa	LDM	3	97	2.26	Viable

*Surgical resection at Day 15.
†Below-knee amputation at 2 yr due to talar osteomyelitis.
‡Above-knee amputation at 2 mo due to proximal tibial osteomyelitis.

fx = fracture; Rect = rectus abdominus free flap; LD = latissimus dorsi free flap; LDM = latissimus dorsi myocutaneous flap; STSG = split thickness skin graft; GSW = gunshot wound.

region of interest (ROI) was scanned. Typically, this region was the center of the wound for patients who free-muscle transfer flap and the distal margin of the wound or affected soft tissue for patients with peripheral vascular disease. Tissue was considered nonviable by visual analysis if it showed little or no FDG uptake, despite the presence of soft tissue on the transmission images.

Semiquantitative image analysis was performed to calculate FDG uptake in the affected muscle region as compared to muscle in the contralateral limb according to the following equation:

$$UR = \frac{\text{study muscle activity (ECAT cps/px)}}{\text{contralateral muscle activity (ECAT cps/px)}},$$

where UR represents the FDG uptake ratio and ECAT cps/px (counts per second per pixel) represents FDG tracer activity concentration in the tissue ROI. Typically, uptake ratios were averaged without pixel weighting from proximal, middle and distal slices to obtain an "average" ratio. Regions of interest were defined on the transmission scan when tissue FDG activity could not be seen clearly on the emission images. Although peripheral vascular disease often affects the extremities bilaterally, we studied patients with probable acute unilateral ischemia and therefore considered the contralateral limb activity to be normal for the uptake ratio calculation. For several patients with peripheral vascular disease, the uptake ratios were calculated only between soft-tissue activity on the injured lower leg or foot and the contralateral side because the clinical ROI was located over the ankle or distal lower leg where skeletal muscle tissue is largely absent.

For patients who had skeletal muscle transfer, FDG uptake ratios were correlated with long-term muscle viability assessed during clinical follow-up. For the patients with peripheral vascular disease, FDG uptake ratios were correlated with wound healing and limb survival or with the surgeon's operative interpretation of tissue viability. Patients who had skeletal muscle transfer were in clinical follow-up for 3 mo to 2 yr. Patients with peripheral vas-

cular disease had follow-up for shorter periods to assess wound healing or need for surgery.

RESULTS

Outcome analysis of the 16 patients with peripheral vascular disease is shown in Table 2. FDG uptake ratios ranged from 0.12 to 1.72 (mean: 1.05 ± 0.37). In six patients, the PET scan demonstrated nonviable tissue with FDG uptake ratios between 0.12 and 0.46 (mean 0.30 ± 0.11), and the ten patients whose PET scans demonstrated viable tissue had FDG uptake ratios ranging between 0.47 and 1.72 (mean: 1.05 ± 0.37; p < 0.05). One patient had an ulcer in the plantar surface of the foot and an FDG uptake ratios of 1.72; the ulcer was healed during her initial hospitalization, but the foot was amputated 3 mo later because of recurrent ulcers. A second PET scan was not performed before her amputation.

Results from 14 patients referred for evaluation of skeletal muscle transfer flap viability within 15 days of surgery are shown in Table 1. Two patients were studied twice during the immediate postsurgical period. No correlation between glucose level and FDG uptake ratio was found in 11 patients. FDG uptake ratios ranged from 0.12 to 7.88 (mean 3.09 ± 2.01; n = 16), with higher values noted in the early postoperative period (Fig. 1). Viable muscle graft FDG uptake ratios ranged from 0.73 to 7.88 (mean 3.23 ± 1.92; n = 15). Two patients ultimately required amputation due to osteomyelitis despite graft viability. Only one patient had nonviable muscle in the immediate postoperative period; his FDG uptake ratio was 0.12 at Day 13.

Three sample cases representing a nonviable myocuta-

TABLE 2
Patients with Peripheral Vascular Disease

Patient no.	Age (yr)	Sex	Clinical diagnosis	Surgical procedure	Glucose (mg/dl)	Uptake ratio	Clinical outcome
1	59	M	Acute occlusion right iliac artery	Thrombectomy	116	0.46	Nonviable
2	75	F	Left foot ulcer	Left femoral-popliteal artery bypass	72	1.16	Viable
3	46	M	Distal aortic thrombus	ABF, thrombectomy	132	0.24	Nonviable
4	90	F	Left superficial femoral artery occlusion	Left femoral-popliteal artery bypass, BKA	111	0.33	Nonviable
5	83	F	Severe posterior tibial artery atherosclerosis	BKA	269	0.12	Nonviable
6	51	M	Right iliac artery occlusion	Right aortoiliac-femoral artery bypass		1.33	Viable
7	46	M	Pelvic fracture	ORIF	144	0.88	Viable
8	60	F	Severe peripheral vascular disease	ABF	155	1.72	Nonviable*
9	68	M	Aortoiliac disease	STSG	99	0.33	Nonviable
10	80	M	Severe venous stasis	dressings	170	0.82	Viable
11	63	F	Peripheral vascular disease + venous stasis	dressings	84	0.47	Viable
12	63	M	Left femoral artery thrombosis	Left femoral-popliteal artery bypass	151	0.56	Viable
13	72	M	Aortoiliac disease	ABF	83	0.79	Viable
14	71	M	Aortoiliac disease	ABF	172	1.04	Viable
15	55	M	Left common femoral artery thrombus	Debridement + STSG ·	139	1.40	Viable
16	45	M	Severe peripheral vascular disease	Left popliteal-posterior tibial artery graft	68	1.29	Viable†

*Extremity healed during initial hospitalization but required amputation 3 mo later for recurrent ulcers.
†Initial surgical revascularization demonstrated good distal extremity healing, but graft clotted at postoperative Day 4 and the patient underwent BKA.
ABF = aortobifemoral bypass; BKA = below-knee amputation; ORIF = open reduction internal fixation; STSG = split thickness skin graft.

neous skeletal muscle transfer graft (Case 1), a viable transfer flap (Case 2) and a nonviable extremity in a patient with peripheral vascular disease (Case 3) are presented below.

Case 1

Figure 2 is the PET scan of Patient 3, a 54-yr-old man who underwent a myocutaneous rectus abdominus transfer flap over the anteromedial midtibia for a nonhealing diabetic ulcer. Clinical evaluation 10 days after surgery demonstrated coolness of the graft to touch despite bleeding to pinprick. The transmission PET scan shows the extent of the transfer graft over the midtibia with absence of FDG activity in the same area. The FDG uptake ratio was 0.12. Note there is evidence of skin activity on the emission scan, which may explain the clinical impression of graft viability by tissue bleeding. Surgical exploration 2 days later confirmed necrosis of the graft.

Case 2

Figure 3 shows the PET scan results of Patient 13, a 22-yr-old man whose scan was obtained 7 mo after traumatic amputation of the right forefoot with recurrent ulcers in a split-thickness skin graft 5 days after latissimus dorsi myocutaneous flap to close the
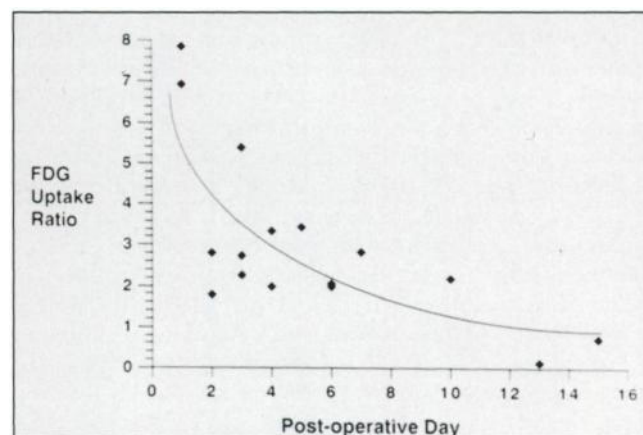

FIGURE 1. Plot of FDG uptake ratio versus days after surgery (n = 16). The solid line is the trend in the viable muscle group. The muscle represented by the point at Day 13 (UR = 0.12) was determined to be nonviable at surgery 2 days after the PET scan.
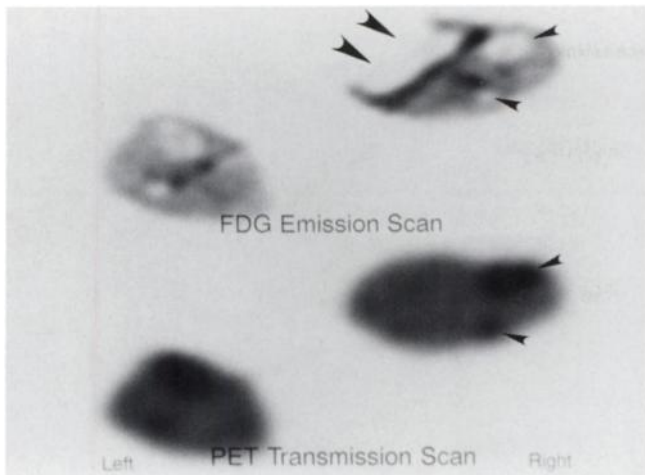
FIGURE 2. PET emission and transmission scans from Patient 3 show nonviable tissue in an anterior tibial skeletal muscle transfer flap (large arrowheads). The tibia and fibula (small arrowheads) visible in both the emission and transmission scans provide cross-sectional anatomic landmarks. Asymmetry in leg orientation results from difficulty with positioning due to postsurgical dressings and immobilization hardware.

open wound. The transmission scan shows the extent of the transfer flap in the lateral right ankle. The FDG emission image shows good uptake of radiotracer in the flap with a curvilinear region of decreased activity deep to the flap, indicating edema or hematoma. This "edema" pattern has been seen in several patients both after free-muscle transfer flap and after trauma with known hematoma. No corrective surgery was necessary to drain the fluid. The FDG uptake ratio in this flap was 2.0. Follow-up to 6 mo after surgery showed continued flap viability.

Case 3

Figure 4A shows an example of a PET scan in Patient 1, a 59-yr-old man who presented with a 5-day history of right leg pain, which had increased on the day of admission. An arteriogram
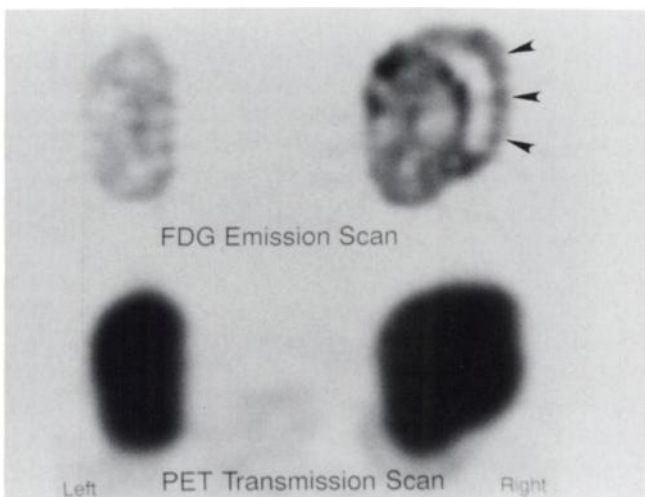

FIGURE 3. PET emission and transmission scans from Patient 13 show good tracer uptake throughout the skeletal muscle transfer flap over the right lateral malleolus (arrowheads). Note the crescentic region of decreased activity deep to the flap, which likely indicates edema or hematoma.
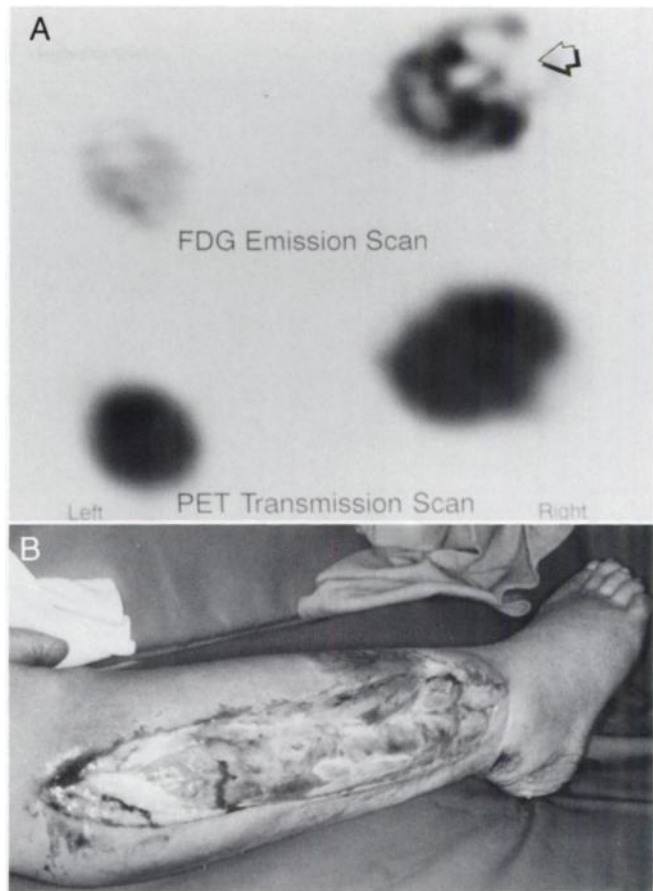

FIGURE 4. (A) PET emission and transmission scans from Patient 1 show decreased tracer uptake in the lateral compartment of the right lower leg (arrow). The uptake ration of 0.46 was consistent with nonviable tissue. (B) The lower leg was amputated because of nonhealing wounds 1 wk after the PET scan.

showed a right iliac artery occlusion. Streptokinase therapy resulted in revascularization of the leg to the level of the popliteal artery. The day following admission, he underwent popliteal thrombectomy and vein patch angioplasty plus fasciotomy. Over the next week, he underwent multiple debridements of the lateral right lower leg along with daily hydrotherapy for treatment of his wound. Seven days after surgery, a PET scan showed presence of tissue in the lateral leg, but no FDG activity in much of the area, suggestive of nonviable tissue. The FDG uptake ratio in the right lateral leg was 0.12. One week after the PET scan, he underwent an above-knee amputation for necrosis of the wound area (Fig. 4B).

DISCUSSION

Various radionuclide techniques have been developed to differentiate nonviable tissue from salvageable tissue in patients with ischemic peripheral vascular disease or injury. These techniques, including measurements of tissue blood flow and perfusion pressure, were developed to reduce the high number of surgical stump revisions in patients whose amputation level was selected by clinical judgment alone (2). Other nonradionuclide tests devised to estimate transcutaneous oxygen tension, transcutaneous carbon dioxide tension, skin temperature and arterial pres-

TABLE 3
Amputation Level Outcome

A. Based on Skin Blood Perfusion Threshold (SBP)			
Investigator (Ref.)	SBP threshold (ml/min/100 g)	Number (%) healed for SBP > threshold	No. (%) failed for SBP < threshold
Moore et al., 1981 (6)	2.4	25/25 (100)	—
Malone et al., 1981 (7)	2.6	35/36 (97)	—
Silberstein et al., 1983 (8)	2.4	38/39 (97)	—
Malone et al., 1987 (11)	NS*		
Harris et al., 1987 (10)	1.0	17/17 (100)	5/5 (100)
Dwars et al., (9)	2.8	26/27 (100)	1/2 (50)

B. Based on Skin Perfusion Pressure Threshold (SPP)			
Investigator (Ref.)	SPP threshold (mmHg)	No. (%) healed for SPP > threshold	No. (%) failed for SPP < threshold
Faris, Donean, 1985 (12)	40	35/40 (88)	20/21 (95)
Holstein, 1985 (13)	20–30	(50%)	
Dwars et al., 1989 (9)	20	26/26 (100)	2/3 (67)

*No significant threshold found.

sure indices based on Doppler ultrasound in patients with peripheral vascular disease have met with varying success (3–5).

Several investigators have measured skin blood flow and skin perfusion pressure to predict the optimal amputation level for patients with peripheral vascular disease (Table 3). Studies by Moore et al. (6), Malone et al. (7), Silberstein et al. (8), and Dwars et al. (9) found that a skin blood flow of 2.4–2.8 ml/min/g predicted a 97%–100% healing rate. In a smaller series, Harris et al. (10) found a threshold of 1.0 ml/min/g. In another series, Malone et al. (11) failed to demonstrate a threshold flow. They thought this may be due to technical limitations in performing the test. Another possibility is that skin blood flow does not reflect perfusion to deeper tissues. This appeared to be true in the patient in our pilot series who showed enhanced NH_3 and FDG tissue uptake in the skin overlying a region of decreased activity in deeper tissue. This patient's wounds healed following prolonged treatment, including hyperbaric oxygen therapy.

Measurement of skin perfusion pressure has also been analyzed in the same way as the skin blood flow threshold (Table 3). Faris and Duncan (12) found an 88% healing rate at amputation levels in which the skin perfusion pressure was greater than 40 mmHg. Dwars et al. (9) reported that a skin perfusion pressure of 20 mmHg was predictive of healing in 26 (100% positive predictive value) patients. Holstein (13) found no reliable skin perfusion pressure threshold. The differences in these studies probably relate to both technical and physiologic factors. It may be necessary for institutions to establish threshold values for skin blood flow and skin perfusion pressure in order to use these tests reliably.

Thallium-201 has been used for imaging both skin and skeletal muscle perfusion and to determine the potential for wound healing in patients with peripheral vascular disease. Siegel et al. (14) derived a skin hyperemia index by dividing the average ^{201}Tl activity in injured tissue by that in the surrounding skin. In a series of 13 diabetic patients with noninfected foot ulcers, he showed that an index of 1.5 or greater was predictive of healing. Ohta (15) described four types of ^{201}Tl image patterns seen in 36 patients with foot ulcers secondary to peripheral vascular disease. Positive uptake in the ulcer bed on both the initial and delayed images was predictive of subsequent healing in 31 of 32 patients. No initial uptake predicted nonhealing in 8 of 13 patients. Oshima et al. (16) described the normal distribution of ^{201}Tl activity using quantitative SPECT scanning in six volunteers. This database was used in a series of patients with peripheral vascular disease, and Oshima found a sensitivity of 92% for detection of angiographically significant lesions. In four of five patients who were misdiagnosed with ^{201}Tl SPECT, the stenosis was proximal and collateral flow was apparently adequate to compensate for the stenosis. Similar analysis of ^{201}Tl muscle kinetics has been used to evaluate arterial occlusive disease (17,18) and exercise-induced vasospastic leg ischemia (19).

Assessment of skeletal muscle viability has been previously evaluated using ^{99m}Tc-pyrophosphate (PYP) imaging. Labbe et al. (20) reported a statistically significant correlation between the extent of muscle necrosis and uptake of ^{99m}Tc-PYP in canine gracilis muscle subjected to graded ischemia. Timmons et al. (21) correctly predicted the level of skeletal muscle necrosis and healing of surgical wounds in 14 of 16 patients undergoing amputation for chronic peripheral vascular disease. In those studies, immediate postinjection scans were performed to estimate tissue perfusion. Delayed images showed various patterns of uptake: (a) normal PYP uptake suggestive of viable, noninjured tissue; (b) increased PYP indicative of injured

tissue with necrosis; and (c) decreased or absent PYP consistent with nonviable necrotic tissue.

Technetium-99m-PYP localizes in skeletal muscle during exertion and rhabdomyolysis. Therefore, these conditions must be excluded prior to image interpretation. Technetium-99m-PYP has been used to evaluate tissue ischemia in acute embolic disease (22), arterial trauma (23), frostbite injury (24) and in electrical burns (25, 26). In these cases, increased PYP may indicate both tissue ischemia and necrosis. SPECT scanning with PYP has been used to quantify the volume of necrotic muscle (27). Several authors have reported the utility of combined ^{201}Tl perfusion imaging and delayed PYP ischemia assessment (28). These techniques are promising for qualitative evaluation of tissue ischemia but, unlike PET, do not allow dynamic scanning with attenuation correction required for quantitation.

Elfner et al. (29) demonstrated the potential of quantifying skeletal muscle blood flow with [82]Rb PET in 10 patients with peripheral vascular disease. Their results suggested that diminished perfusion flow reserve (defined as the ratio of calculated postocclusive hyperemic skeletal muscle blood flow and resting skeletal muscle blood flow) was predictive of a significant proximal arterial stenosis, but they did not attempt to determine muscle viability or predict surgical outcome.

We used FDG-PET scanning with semiquantitative analysis of attenuation corrected images to determine muscle viability in patients with complications of peripheral vascular disease or following free-flap skeletal muscle transfer. For all patients, viable muscle uptake ratios ranged from 0.47 to 7.88 (mean 2.26 ± 1.81; n = 26), while nonviable muscle uptake ratios ranged from 0.12 to 0.46 (mean 0.27 ± 0.12; n = 6; p < 0.02). The wide range of viable tissue uptake ratios reflects the effect of reduced blood flow or hyperemia on tracer delivery to injured muscle. These values ranged from 0.47 to 1.40 in patients with peripheral vascular disease who had viable muscle. In patients with viable tissue after free-flap transfer, higher URs are seen in the early postoperative period (mean 4.59 ± 2.46; range 1.77–7.88 at Days 0–3; n = 7) than in the later period (mean 2.33 ± 0.89; range 0.73–3.47; days 4–15; n = 8) reflecting hyperemia during that time (Fig. 1).

One patient with peripheral vascular disease patient who had viable muscle had an FDG uptake ratio of 0.47. This patient required prolonged medical therapy, including hyperbaric oxygen therapy, to finally heal his wounds. The remaining FDG uptake ratios in the viable muscle group were all greater than 0.50 (Fig. 5). It is clear from Figure 5 that the accuracy for detection of viable muscle is 100% when the threshold FDG uptake ratio is 0.46. A clinically realistic threshold of 0.5 yields sensitivity and specificity of 96% (25/26) and 100% (6/6), respectively, for PET documented viability. The corresponding positive and negative predictive values are then 100% (25/25) and 86% (6/7), respectively.

In this series, 2 of 13 patients with viable skeletal muscle transfer grafts required amputation due to osteomyelitis. In
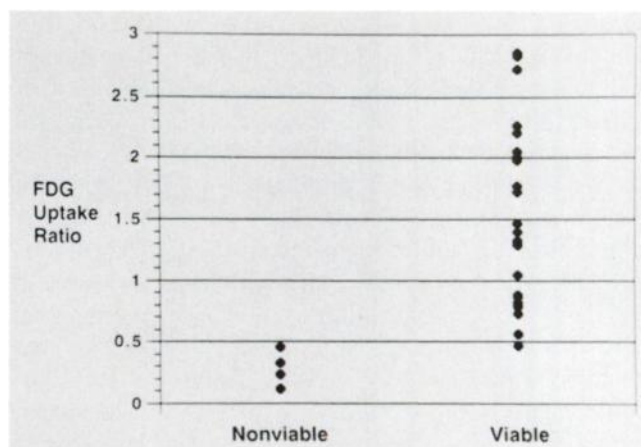

FIGURE 5. FDG uptake ratios for peripheral vascular disease and skeletal muscle transfer nonviable (n = 6) and viable muscle (n = 26) groups as defined by the clinical outcome. All muscles with uptake ratios above 3.0 were viable and are not shown in the graph. The nonviability threshold is 0.46. Patients with ratios below this value ultimately required debridement or amputation; patients with ratios above this value had viable muscles with tissue. One patient with peripheral vascular disease, and an FDG uptake ratio of 1.72, who is included in the viable group, had ulcers that healed during the initial hospitalization but underwent distal extremity amputation for recurrent ulcers 3 mo later. One patient with viable muscle and an FDG uptake ratio of 0.47 required extensive medical therapy for salvage.

one patient, the bony infection was located at a site remote to the graft and could not be inspected during the PET scan. In the other patient, the infected site was located within the field of view but retrospective image analysis revealed no clear distinction between osteomyelitis and postoperative hyperemia.

There was one patient with peripheral vascular disease who had a below-knee amputation for recurrent ulcers 3 mo after PET imaging, which predicted viable tissue by demonstrating good FDG uptake in the soft tissue surrounding her ulcer (FDG uptake ratio = 1.72). Unfortunately, a repeat PET scan prior to surgery could not be obtained. This case was considered to represent viable tissue in the statistical data presented above, but an argument could be made that this represented a false-positive PET scan. If this patient is included in the nonviable group, the positive predictive value for tissue viability is reduced from 100% to 96% (24/25).

In the clinical setting, differentiating viable from nonviable tissue in patients with peripheral vascular disease is often difficult. We used the surgeon's description of the tissue for evidence of nonviability in the patients who underwent debridement or amputation. A more rigorous approach would be to use histologic analysis of the muscle for evidence of nonviability according to the method of Labbe et al. (30). Nevertheless, clinical correlation and outcome define the utility of the method in daily practice. By this criterion, we believe the analytical methods reported in this article are useful for this initial investigation.

In this study, we attempted to limit the analysis to re-

gions containing skeletal muscle. While it was difficult to include only skeletal muscle for some patients, we did not analyze simple skin activity over ulcer beds. Utilization of FDG-PET to evaluate the healing potential of ulcers will require subsequent studies. Because we did not look specifically at skin activity, comparison of FDG-PET with other modalities is problematic, but our overall impression suggests that PET offers improved diagnostic accuracy for detecting viable and nonviable tissues. This is likely due to the ability to construct transaxial images representing three-dimensional tracer distribution and to correct for attenuation artifacts with PET. These features of PET provide a relatively simple method to quantitate FDG uptake in the tissues. Also, the use of arterial blood sampling in PET provides a method for quantifying FDG metabolism in an absolute sense (e.g., mg ^{18}F-glucose consumed/min/g tissue), but this is obviously more invasive, requires more extensive data processing and is less practical for routine clinical use.

The cost for this type PET study approaches $1500 per scan and takes 1–2 hr. These factors are considerable compared to simple clinical evaluation of tissue viability. For selected patients in whom surgical intervention is a consideration or prolonged hospitalization for observation may be required, we believe PET can be a cost-effective method of defining the presence and extent of nonviable tissue.

CONCLUSION

This article outlines an approach using FDG-PET scanning to assess skeletal muscle viability both in patients with free-flap muscle transfer, and complications of peripheral vascular disease. The method appears to be highly accurate to assess the metabolic state of the muscle at the time of the scan and may offer prognostic information for long-term outcome. This technique may play an important role in postsurgical evaluation of complicated muscle grafting and in the preoperative assessment of tissue viability in patients with peripheral vascular disease.

ACKNOWLEDGMENT

REFERENCES

1. Padgett HC, Schmidt DG, Luxen A, et al. Computer-controlled radiochemical synthesis: a chemistry process control unit for the automated production of radiochemicals. *Appl Radiat Isot* 1989;40:433–445.
2. Keagy BA, Schwartz GA, Kotb M, et al. Lower extremity amputation: the control series. *J Vasc Surg* 1986;4:321–326.
3. Onishi CS, Fronek A, Golbranson FL. The role of noninvasive vascular studies in determining levels of amputation. *J Bone Joint Surg* [Am] 1988; 70-A:1520–1530.
4. Welch GH, Leiberman DP, Pollock JG, Angerson W. Failure of Doppler ankle pressure to predict healing of conservative forefoot amputations. *Br J Surg* 1985;72:888–891.
5. Harrison DH, Girling M, Mott G. Methods of assessing the viability of free
flap transfer during the post-operative period. *Clin Plastic Surg* 1983;10:21–36.
6. Moore WS, Henry RE, Malone JM, et al. Prospective use of Xe-133 clearance for amputation level selection. *Arch Surg* 1981;116:86–88.
7. Malone JM, Leal JM, Moore WS, et al. The "gold standard" for amputation level selection: xenon-133 clearance. *J Surg Res* 1981;30:449–455.
8. Silberstein EB, Thomas S, Clive J, et al. Predictive value of intracutaneous xenon clearance for healing of amputation and cutaneous ulcer sites. *Radiology* 1983;147:227–229.
9. Dwars BJ, Rauwerda JA, van den Broek TAA, et al. A modified scintigraphic technique for amputation level selection in diabetics. *Eur J Nucl Med* 1989;38–41.
10. Harris JP, McLaughlin AF, Quinn RJ, et al. Skin blood flow measurement with xenon-133 to predict healing of lower extremity amputations. *Aust NZ J Surg* 1987;56:413–415.
11. Malone JM, Anderson GG, Lalka SG, et al. Prospective comparison of noninvasive techniques for amputation level selection. *Am J Surg* 1987;154: 179–184.
12. Faris I, Duncan H. Skin perfusion pressure in the prediction of healing in diabetic patients with ulcers or gangrene of the foot. *J Vasc Surg* 1985;2: 536–540.
13. Holstein E. Skin perfusion pressure measured by radioisotope washout for predicting wound healing in lower limb amputation for arterial occlusive disease. *Acta Orthop Scand Suppl* 1985;56:4–47.
14. Siegel ME, Stewart CA, Wagner FW Jr, Sakimura I. An index to measure the healing potential of ischaemic ulcers using thallium-201. *Prosth Orthot Int* 1983;7:67–68.
15. Ohta T. Noninvasive technique using thallium-201 for predicting ischaemic ulcer healing of the foot. *Br J Surg* 1985;72:892–895.
16. Oshima M, Akanabe H, Sakuma S, et al. Quantification of leg muscle perfusion using thallium-201 single photon emission computed tomography. *J Nucl Med* 1989;30:458–465.
17. Chevreaud C, Thouvenot P, Lapeyre G, et al. Thallium 201 muscle scintigraphy: application to the management of patients with arterial occlusive disease. *J Vasc Dis* 1987;309–314.
18. Earnshaw JJ, Hardy JG, Hopkinson BR, Makin GS. Non-invasive investigation of lower limb revascularisation using resting thallium peripheral perfusion imaging. *Eur J Nucl Med* 1986;12:443–446.
19. Hartshome MF, Peters V, Williams RD, et al. Vasospastic exercise-associated unilateral leg ischemia: evaluation with thallium-201. *Am J Phys Imaging* 1987;2:82–84.
20. Labbe R, Lindsay T, Walker PM. The extent and distribution of skeletal muscle necrosis after graded periods of complete ischemia. *J Vasc Surg* 1987;6:152–157.
21. Timmons JH, Hartshome MF, Peters VJ, et al. Muscle necrosis in the extremities: evaluation with ^{99m}Tc pyrophosphate scanning-A retrospective review. *Radiology* 1988;167:173–178.
22. Moss CM, Delany HM, Rudavsky AZ. Isotope angiography for detection of embolic arterial occlusion. *Surg Gynecol Obstet* 1976;142:57–61.
23. Moss CM, Veith FJ, Jason R, et al. Screening isotope angiography in arterial trauma. *Surgery* 1979;19:409–413.
24. Purdue GF, Lewis SA, Hunt JL. Pyrophosphate scanning in early frostbite injury. *Am Surg* 1983;49:619–620.
25. Hunt J, Lewis S, Parkey R, et al. The use of Tc-99m stannous pyrophosphate scintigraphy to identify muscle damage in acute electrical burns. *J Trauma* 1979;19:409–413.
26. Spencer RR, Williams AG Jr, Mettler FA Jr, et al. Technetium-99m PYP scanning following low voltage electrical injury. *Clin Nucl Med* 1983;8:591–593.
27. Forrest I, Hayes G, Smith A, Yip TCK, Walker PM. Identification of clinically significant skeletal muscle necrosis by single photon emission computed tomography. *Can Soc Vasc Surg* 1989;32:109–112.
28. Kaufman JL, Deak ST, Erdman W. Radionuclide scans to define patterns of occult myonecrosis. *NJ Med* 1986;83:101–103.
29. Elfner R, Henrich MM, Theiss A, et al. Assessment of regional skeletal muscle perfusion with rubidium-82 PET [Abstract]. *J Nucl Med* 1993; 34(suppl):87P.
30. Labbe R, Lindsey T, Gatley R, et al. Quantitation of post-ischemic skeletal muscle necrosis: histochemical and radioisotope techniques. *J Surg Res* 1988;44:45–53.